References and Notes

(1) *Polymer Blends*; Paul, D. R., Newman, S., Eds.; Academic Press: New York, 1978.
(2) Olabisi, O.; Robeson, L. M.; Shaw, M. T. *Polymer-Polymer Miscibility*; Academic Press: New York, 1978.
(3) Goh, S. M.; Paul, D. R.; Barlow, Y. W. *J. Appl. Polym. Sci.* **1982**, *27*(3), 1091.
(4) Fayt, R.; Jerome, R.; Teyssie, P. *J. Polym. Sci., Polym. Lett.* **1981**, *19*, 79.
(5) Djadoun, S.; Goldberg, R. N.; Morawetz, H. *Macromolecules* **1977**, *10*, 1015.
(6) Pearce, E. M.; Kwei, T. K.; Min, B. Y. *J. Macromol. Sci., Chem.* **1984**, *A21*, 1181.
(7) Pugh, C.; Percec, V. *Macromolecules* **1986**, *19*, 65.
(8) Prud'homme, R. E. *Polym. Eng. Sci.* **1982**, *22*, 90.
(9) Hara, M.; Eisenberg, A. *Macromolecules* **1984**, *17*, 1335.
(10) Smith, P.; Eisenberg, A. *J. Polym. Sci., Polym. Lett. Ed.* **1983**, *21*, 223.
(11) Murali, R.; Eisenberg, A. *J. Polym. Sci., Part B: Polym. Phys.* **1988**, *26*, 1385.
(12) Douglass, D. C.; McBrierty, V. J. *Macromolecules* **1978**, *11*, 766.
(13) Caravatti, P.; Neuenschwander, P.; Ernst, R. R. *Macromolecules* **1986**, *19*, 1889.
(14) Henrichs, M. P.; Tribone, J.; Massa, D. J.; Hewitt, J. M. *Macromolecules* **1988**, *21*, 1282.
(15) Ward, T. C.; Lin, T. S.; *ACS Symp. Ser.* **1984**, *No. 206*, 59.
(16) Schaefer, J.; Sefcik, M. D.; Stejskal, E. O.; Mckay, R. A. *Macromolecules* **1981**, *14*, 188.
(17) Parmer, J. F.; Dickinson, L. C.; Chien, J. C. W.; Porter, R. S. *Macromolecules* **1987**, *20*, 2308.
(18) Gobbi, G. C.; Silvestri, R.; Russell, T. P.; Lyerla, J. R.; Fleming, W. W.; Nishi, T. *J. Polym. Sci., Part C: Polym. Lett.* **1987**, *25*, 61.
(19) Krause, S. In *Polymer Blends*; Paul, D. R., Newman, S. Eds.; Academic Press: New York, 1978; *Vol. 1*, p 75.
(20) Natansohn, A.; Eisenberg, A. *Macromolecules* **1987**, *20*, 323.
(21) Makowski, H. S.; Lundberg, R. D.; Singhal, G. H. U.S. Patent 3,870,841, 1975.
(22) Duchesne, D. Ph.D. Thesis, McGill University, 1985.

Registry No. (PMMA)(4VP) (copolymer), 26100-41-4; (PMMA)(4VP)·CH_3I (copolymer), 110923-53-0; $N(CH_3)_4OH$, 75-59-2.

Hydrostatic Pressure Dependence of Molecular Motions in Polycarbonates

J. H. Walton, Martin J. Lizak, and Mark S. Conradi

Department of Physics, Washington University, St. Louis, Missouri 63130

Terry Gullion and Jacob Schaefer*

Department of Chemistry, Washington University, St. Louis, Missouri 63130.

Received September 15, 1988; Revised Manuscript Received June 26, 1989

ABSTRACT: The temperature dependence of the proton NMR line width of polycarbonate and of the phenoxy resin formed from bisphenol A and epichlorohydrin have been measured as a function of hydrostatic pressure. These measurements lead to the conclusion that for both polymers, ring motions are suppressed by the denser chain packing resulting from hydrostatic pressure. The magnitude of the NMR pressure dependence is comparable to the pressure variation of the γ mechanical loss peak in polycarbonate. The ^1H NMR results, together with those from a variety of cross-polarization magic-angle spinning ^{13}C NMR experiments performed at room temperature and atmospheric pressure, are interpreted in terms of a bundle model of chain packing in the glassy matrix. From the observed activation volumes, activation energies, and main-chain reorientation rates, the bundles are inferred to involve the correlated motions of just a few chains.

Introduction

Polycarbonate (PC) forms a glassy polymer that is remarkable for its high-impact resistance and ductility over a wide temperature range. Molecular motions occurring below T_g have long been believed to be at least partly responsible for PC's favorable mechanical properties.[1] Indeed, a substantial mechanical loss peak ("γ") observed in PC indicates the presence of 1-Hz motions (which are coupled to bulk and shear modes) 250 °C below T_g.

Nuclear magnetic resonance (NMR) has been used to assemble a picture of the motions present in polycarbonate. Deuterium NMR line shapes,[2] ^{13}C chemical shift anisotropy patterns,[3] and ^{13}C–^1H dipolar spectra[4] have yielded the most specific information. The most obvious motions in the NMR spectra are 180° flips of the phenylene groups about their C_2 axes and methyl rotations about the C_3 axes. Because these motions carry the molecule back into itself, they cannot be directly responsible for the mechanical loss and favorable mechanical properties of PC. However, the rate of phenylene 180° flips does appear on the same temperature–frequency relaxation line with the γ mechanical and dielectric loss peaks.[5] Closer examination of the ^{13}C–^1H dipolar spectra of phenylene and methyl carbons indicates that other motions are also present at room temperature:[6] these include approximately 30° oscillations of the phenylene groups about the C_2 axes and 15° main-chain reorientations ("wiggles"). It has been proposed[7] that the main-chain motions create sufficient volume to enable, or gate, the 180° ring flips. Thus, the ring flips are an indirect measure of the mechanically active main-chain motions.

In this paper, we establish a link between the NMR measurements and the mechanically active motions. The mechanically active motions (specifically, the bulk modes) necessarily produce volume fluctuations that can be probed by changing the conjugate variable, pressure.[8,9] Thus, we have measured the temperature and pressure dependence up to 1800 bars of the proton T_2 in PC and in the phenoxy resin of bisphenol A and epichlorohydrin (PK). Because proton NMR measurements often are unable to specify the exact nature of motions present, our interpretation of motion is based on the high-pressure proton

0024-9297/90/2223-0416$02.50/0

results in combination with results from ^{13}C T_1, $T_{1\rho}$, and dipolar rotational spin-echo experiments at atmospheric pressure.

Experimental Section

High-Pressure Proton NMR Experiments. Polymer samples were pressurized in a titanium alloy vessel with a ratio of outer to inner diameters of 4. The sample of 2-mm diameter and 2-cm length was surrounded by a rf solenoid of fluorocarbon insulated wire (Bio-med wire, Cooner Wire, Chatsworth, CA). The insulated wire continued to ambient temperature through the high-pressure stainless piping. The radio-frequency wire was passed to ambient pressure by a room-temperature feed-through made of ceramic-insulated, sheathed, thermocouple wire impregnated by molten candle wax under pressure. The outer jacket of the thermocouple wire was hard-soldered to a standard, drilled, high-pressure cone fitting. This worked well at the proton operating frequency of 21.3 MHz.

The samples were pressurized up to 1800 bars (1.013 bar = 1 atm) with helium gas. Helium (rather than a safer liquid pressure agent) was chosen to avoid dissolving the polymer sample. Helium also minimizes the changes due to solvent uptake under pressure. The solubility of He in PC at room temperature and 1800 bar is about 0.2% (by weight).[10] Helium from a cylinder at 150 bars was purified with a liquid-nitrogen trap and an Oxisorb cartridge (MG Industries). Pressure was generated with an Aminco diaphragm compressor driven by an Aminco oil pump. Pressures were measured with a Heise Bourdon tube gauge.

Temperature control was provided by a thermostated stream of N_2 gas, obtained by boiling liquid nitrogen. The pressure vessel and about 12 cm of piping above it were located in a glass-tube Dewar, promoting temperature homogeneity. The temperature was determined with a thermocouple. Temperatures did not exceed T_g of the polymer examined.

Magic-Angle Spinning and ^{13}C NMR Relaxation Measurements. Cross-polarization magic-angle spinning ^{13}C NMR spectra were obtained at room temperature on a spectrometer built around a 12-in. iron magnet operating at a proton Larmor frequency of 60 MHz.[11] Half-gram samples were spun in a double-bearing rotor[12] at 1859 or 930 Hz. $T_1(C)$ was measured by the Torchia method[13] and $T_{1\rho}(C)$ by standard procedures.[14]

Carbon Dipolar Sideband Patterns. Carbon dipolar line shapes were characterized by dipolar rotational spin-echo ^{13}C NMR at 15.1 MHz. This is a two-dimensional experiment[15] in which, during the additional time dimension, carbon magnetization is allowed to evolve under the influence of H–C coupling while H–H coupling is suppressed by homonuclear multiple-pulse, semiwindowless MREV-8 decoupling.[16] The cycle time for the homonuclear decoupling pulse sequence was 33.6 μs, resulting in decoupling of proton–proton interactions as large as 60 kHz. Sixteen MREV-8 cycles fit exactly in one rotor period so that strong dipolar echoes formed. A 16-point Fourier transform of the intensity of any peak resolved by magic-angle spinning in the chemical-shift dimension yielded a 16-point dipolar spectrum, scaled by the MREV-8 decoupling, and broken up into sidebands by the spinning.[4]

Materials. The PC used in the ^{13}C experiments was obtained as Lexan pellets, manufactured by General Electric. The PK was a former commercial product of Union Carbide designated as PKHH resin.[17] Thin sheets of PC and PK were melt pressed above T_g and annealed by slow cooling to room temperature in the press. The ^{13}C NMR samples consisted of stacks of thin disks cut from sheets. The PK used in the high-pressure proton measurements consisted of several small pieces chipped from a sheet. The high-pressure proton PC sample was machined from Lexan rod. A specifically deuterated PC was prepared by R. J. Kern (Monsanto Co., St. Louis, MO) from monomer supplied by Merck, Canada. The molecular weight of the specifically deuterated PC was 40 000; the sample was examined as a powder.

Results

Proton NMR Line Widths as a Function of Pressure. A convenient measure of the proton reciprocal line width is the transverse dephasing time, T_2. Because the free induction decay (FID) changes shape with temperature, it is inappropriate to fit the FID to a specific analytical form. Instead, we define T_2 by the relation

$$T_2 \equiv \int_0^\infty [g(t)/g(0)]\, dt \qquad (1)$$

where $g(t)$ is the FID. The above definition is suggested by dimensional arguments and is commonly used in discussions of correlation functions.[18] For an exponentially decaying $g(t)$, the T_2 of eq 1 equals the exponential decay constant.

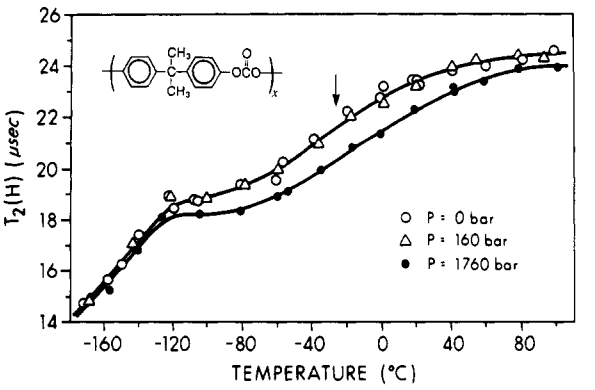

Figure 1. Temperature dependence of the ^1H T_2 of polycarbonate (PC) for three values of the external hydrostatic pressure. The solid lines suggest trends in the data. The arrow indicates the approximate center of the pressure-dependent line-narrowing process.

In practice, our definition of T_2 is slightly different. First, the integral is not extended to infinity but is terminated after $g(t)$ has decayed into the noise. Second, because of receiver dead time following the rf excitation pulse, the early time data are unavailable. Therefore zero time in eq 1 is taken as the earliest time for which the receiver has recovered, approximately 10 μs after the pulse. Shifting the origin of time produces no change in T_2 determined by eq 1 for exponentially decaying FIDs. For Gaussian or nearly Gaussian shapes, the time shift systematically reduces T_2. For consistency, in our experiments, the time shift was held constant.

The proton T_2 of commercial polycarbonate is displayed in Figure 1 and increases by about a factor of 2 between −170 and 80 °C. In the low-temperature region between −170 and −120 °C, T_2 increases with temperature but is unaffected by pressure. This suggests a motion with a zero or small activation volume, such as a C_3 methyl group rotation. This sort of motion is consistent with the absence of low-temperature narrowing in a specifically deuterated PC with protons only in the 3-, 3′-, 5-, and 5′-positions (Figure 2). In previous studies of proton NMR in PC, Falcone and McCall[19] and Davenport and Manuel[20] interpreted line narrowing near −160 °C as due to methyl rotation.

A pressure-dependent process occurs for both the commercial and selectively deuterated PC at temperatures from −100 to 60 °C (Figures 1 and 2). A pressure of 1760 bars produces a 30 °C shift in the variation of T_2 with temperature. If the shift is linear with pressure, no discernible shift is expected at 160 bars, and none is evident in Figure 1. At all temperatures below T_g the effect of pressure upon T_2 was reversible. No pressure-induced crystallization was observed. These results are consistent with the observations of Zoller,[21] who found that PVT relationships for polycarbonate glasses were independent of path in the P–T plane as long as measurement conditions were below T_g.

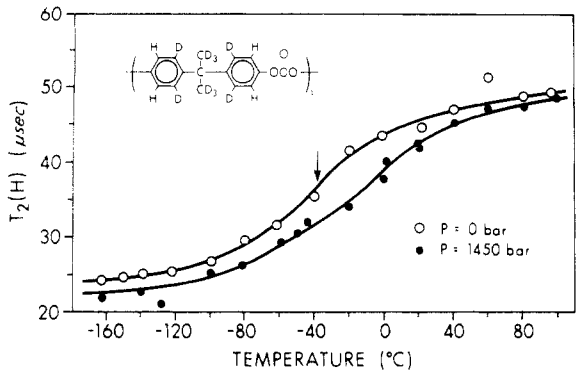

Figure 2. Temperature dependence of the ^1H T_2 of [3,3′,5,5′-$^1H_4$]polycarbonate-d_{10} for two values of the external hydrostatic pressure. The solid lines suggest trends in the data. The arrow indicates the approximate center of the pressure-dependent line-narrowing process.

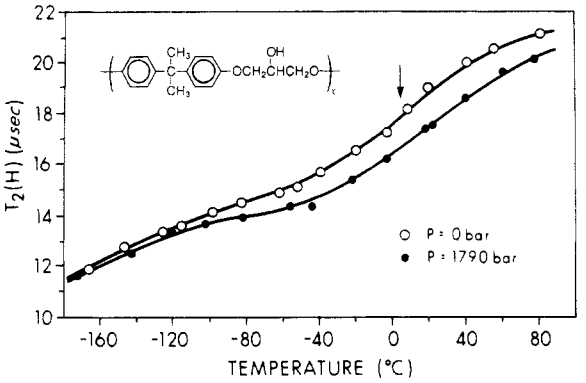

Figure 3. Temperature dependence of the ^1H T_2 of the phenoxy resin formed from bisphenol A and epichlorohydrin (PK) for two values of the external hydrostatic pressure. The solid lines suggest trends in the data. The arrow indicates the approximate center of the pressure-dependent line-narrowing process.

The behavior of the proton T_2 in PK is displayed in Figure 3 and is generally similar to that in PC, although a few differences appear. The low-temperature, pressure-independent narrowing process is less pronounced in PK than in PC and extends over a wider temperature range. The pressure-dependent narrowing process is also broader, starting at −100 °C and extending all the way to T_g (100 °C). A pressure of 1790 bars shifts the T_2 curve of PK by 25 °C, slightly less than the shift for PC.

Activation Energies and Volumes. In all three polymers examined, the line narrowing (i.e., above −120 °C) occurs over a broad temperature range, evidence of site heterogeneity and a broad distribution of activation energies.

The rate, ω, of a thermally activated motion at zero pressure is

$$\omega = \omega_0 e^{-\Delta E/kT} \tag{2}$$

The attempt frequency,[22] ω_0, is approximately 10^{13} s^{-1}. In general, motion will begin to narrow the line[23] when ω is about equal to the rigid-lattice line width, $\omega \cong 10^5$ s^{-1}. Thus, the value of $\Delta E/kT$ will be about 18 at the onset of narrowing. When a distribution of activation energies describes a particular motion, we define a temperature, T^*, at which T_2 is halfway between its high- and low-temperature limits. For example, for PC in Figure 1 reasonable limits are −100 and 80 °C, thus excluding the region of narrowing associated with methyl rotations. From the values of T_2 at the two "plateaus" one finds T^* = 247 K for PC and T^* = 276 K for PK. These temperatures are shown by short vertical arrows in Figures 1–3. The uncertainties in T^* are at least ±10 K. In PK the narrowing from methyl rotations is not fully separated from that by the higher temperature motions. The values of T^* yield weighted mean activation energies, ΔE, obtained from $\Delta E = 18\,kT^*$; the ΔE values for PC and PK are presented in Table I.

Table I
Relaxation Parameters for PC and PK

parameter	polymer PC	PK
$\langle T_1(H)\rangle$,[a] ms	50	60
temp of center of pressure-dependent T_2(H) narrowing process, K	247	276
ΔE, kJ/mol	38	42
ΔV, cm^3/mol	25	20
temp of sub-T_g max in tan δ_G,[b] K	170	210
protonated aromatic $\langle T_1(C)\rangle$,[c] ms	110	190
methyl $\langle T_1(C)\rangle$,[c] ms	58	50

[a] 21.3 MHz, 25 °C. [b] 1 Hz. [c] 50.3 MHz, 25 °C. The cited values are least-squares fits to the initial 10% relaxation. See Figure 6.

The pressure dependence of a thermally activated motion obeys[8]

$$\omega = \omega_0 e^{-(\Delta E + P\Delta V)/kT} \tag{3}$$

The activation volume, ΔV, may be regarded as the physical expansion of the system at the saddle-point configuration[24] or simply as the pressure dependence of the activation energy. The effect of increasing the external pressure can be described as a shift, ΔT, of the region of narrowing to higher temperatures. According to eq 3, application of pressure is equivalent to increasing ΔE; this will shift the middle of the narrowing region to a temperature $T^* + \Delta T$. Thus, we have

$$\Delta E + P\Delta V = 18k(T^* + \Delta T) \tag{4}$$

Because $\Delta E = 18kT^*$, we find that

$$P\Delta V = 18k\Delta T \tag{5}$$

Values of ΔV deduced from the ΔT shifts are 25 cm^3/mol for PC and 20 cm^3/mol for PK (Table I). Analysis of the noisier proton T_2 data from selectively deuterated PC (Figure 2) yields values of T^* = 235 K and ΔT = 25 K, similar to the values found for commercial PC.

^{13}C Spin–Lattice Relaxation. The CPMAS ^{13}C NMR spectrum of PK is well resolved, with four lines observed for the protonated carbons (Figure 4). The oxygenated aliphatic carbon line at 70 ppm is a combination of methylene and methine carbon contributions. The spectrum of PC is similar (data not shown), except, of course, the oxygenated carbon in PC is a carbonyl whose resonance is not resolved from that of the nonprotonated aromatics.[25]

The protonated aromatic carbon T_1 decays of PC and PK (Figure 5) deviate from a straight line, reflecting the dynamic heterogeneity of the glassy state with different relaxation rates associated with different sites in the lattice.[6,25] This heterogeneity is also evident in the methyl carbon T_1 plots (Figure 6). The T_1 relaxation rate of the aromatic carbons of PK is less than that of PC, while the reverse is true for the methyl carbons (Table I).

Dynamic heterogeneity is also evident in the nonlinearity of $T_{1\rho}$ plots for both aromatic and methyl carbons of PC and PK (Figure 7). The H_1(C) dependence of these relaxation rates is extremely weak (Table II), ruling out the possibility of significant contributions to relaxation

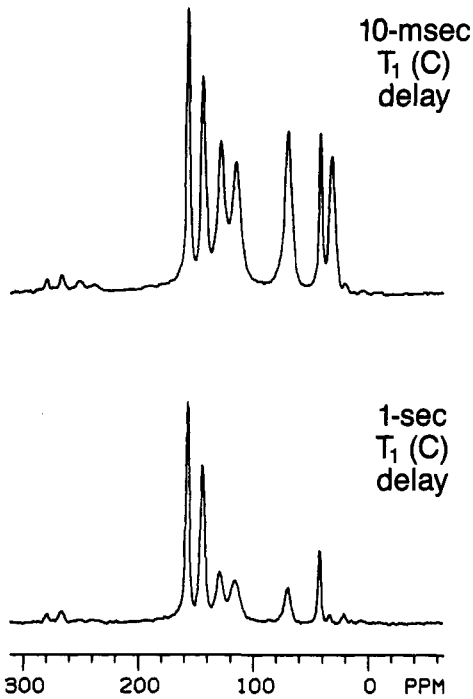

Figure 4. 15.1-MHz CPMAS ^{13}C NMR spectra of the phenoxy resin, PK, after a 10-ms $T_1(C)$ delay (top) and a 1-s $T_1(C)$ delay (bottom). Following cross-polarization, the ^{13}C magnetization is restored to the H_0 direction. After a variable-delay period, designated as the $T_1(C)$ delay, the magnetization is sampled by a 90° pulse. Magic-angle spinning was at 1859 Hz.

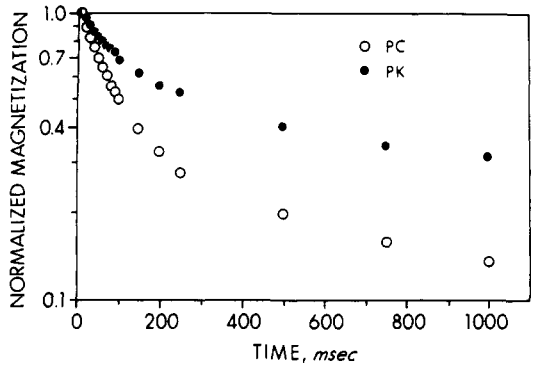

Figure 5. Plot of the $T_1(C)$ relaxation at 15.1 MHz and room temperature of the protonated aromatic carbons of polycarbonate (open circles) and of the phenoxy resin, PK (solid circles).

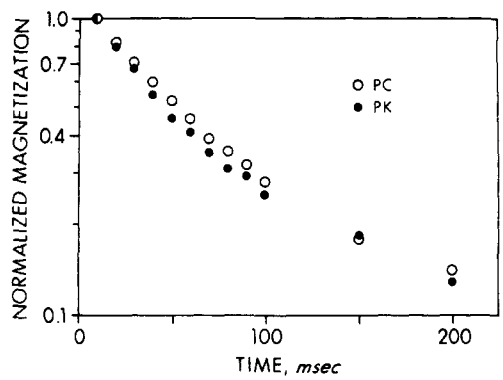

Figure 6. Plot of the $T_1(C)$ relaxation at 15.1 MHz and room temperature of the methyl carbons of polycarbonate (open circles) and the phenoxy resin, PK (solid circles).

from spin–spin processes unrelated to molecular dynamics. The independence of the shapes of the $T_{1\rho}(C)$ plots on $H_1(C)$ for both the methyl and aromatic carbons of PC[26] proves that even minor spin–spin contributions to

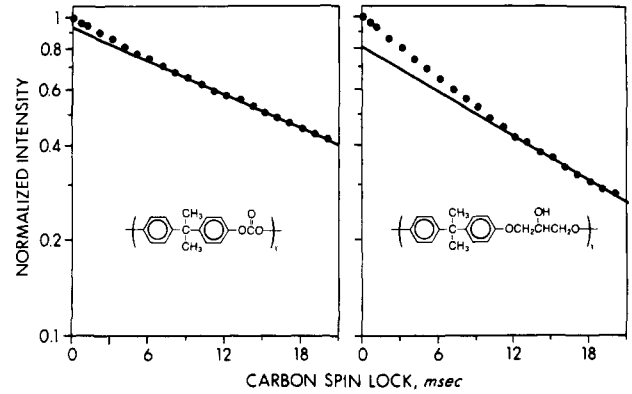

Figure 7. Plots of the $T_{1\rho}(C)$ relaxation at 32 kHz and room temperature of the methyl carbons of polycarbonate (left) and the phenoxy resin, PK (right). The pronounced nonlinearity of the PK plot is the result of the site heterogeneity of main-chain reorientations.

Table II
Radio-Frequency Field Dependence of $T_{1\rho}(C)$[a] for PC and PK

	$\langle T_{1\rho}(C)\rangle$, ms			
	PC		PK	
$H_1(C)$, kHz	methyl	aromatic	methyl	aromatic
32	20	6.5	13	3.0
37	22	6.7	16	3.1
44	27	7.1	18	3.4
50	25	7.5	20	3.2
60	24	7.4	24	4.0

[a] Least-squares fit to the observed decay between 0.05 ms after the turnoff of $H_1(H)$ and 1.00 ms for both protonated aromatic carbon and methyl carbon relaxation at 25 °C.

$T_{1\rho}(C)$ are not present.[27] Theoretical[28] and experimental[26,27] estimates of spin–spin contributions to $T_{1\rho}^{-1}(C)$ for the protonated aromatic carbons of PC are of the order of $(1\ s)^{-1}$, some 2 orders of magnitude less than the observed relaxation rate (Table I). The spin–spin relaxation mechanism is unimportant in PC and PK at room temperature because of the relatively low density of protons in these polymers and because of the averaging of ^1H–^1H dipolar coupling by large-amplitude, high-frequency molecular motions.[14,29] In general, the $T_{1\rho}(C)$ relaxation of PK is faster than that of PC for both aromatic and methyl carbons (Table II).

^1H–^{13}C Dipolar Line Shapes. The large-amplitude motions of the rings in PC that help to reduce the contribution of spin–spin coupling to $T_{1\rho}(C)$ also produce a dipolar line shape with a width only about half that of a conventional ^1H–^{13}C Pake doublet.[4] Thus, the centerband of the aromatic carbon dipolar line shape is stronger than any of the sidebands (Table III). Both aromatic and methyl carbon dipolar and chemical-shift line shapes have been analyzed in detail before,[6] leading to the conclusions that all the rings in PC undergo three types of motions (C_2 flips, C_2 oscillations, and non-C_2 wiggles) and that all the methyls undergo two types of motions (C_3 rotations and non-C_3 wiggles).

These line shapes are only modestly changed when $T_1(C)$ relaxation is used to prepare the carbon magnetization whose dipolar evolution is to be observed. For example, the ratio of intensities of the second to first aromatic carbon dipolar sidebands is 0.504 for the 42% of the population with the fastest $T_1(C)$ relaxation and 0.507 for the 58% of the population with the slowest $T_1(C)$ relaxation (Table III). The methyl carbon dipolar line shape is similarly insensitive to population selection by $T_1(C)$ (Table III).

Table III
Dipolar Rotational Sideband Intensities for PC and PK

polymer	carbon	selection	sideband number 0	1	2	3	4	5	6
PC	protonated aromatic[a]	fastest 42%[b]	0.230	0.227	0.114	0.039	0.009	0	0
		slowest 58%[b]	0.274	0.205	0.104	0.037	0.011	0.005	0.001
PC	methyl[c]	fastest 40%[d]	0.194	0.194	0.116	0.045	0.031	0.012	0.004
		slowest 60%[d]	0.214	0.198	0.114	0.047	0.021	0.012	0.002
PK	protonated aromatic[a]	fastest 25%[b]	0.344	0.236	0.087	0.005	0	0	0
		slowest 75%[b]	0.151	0.163	0.135	0.070	0.030	0.016	0.010
		slowest 50%[e]	0.138	0.152	0.156	0.069	0.036	0.015	0.002
PK	methyl[c]	fastest 50%[d]	0.146	0.181	0.137	0.060	0.034	0.015	0
		slowest 50%[d]	0.231	0.201	0.103	0.035	0.022	0.012	0.011

[a] Magic-angle spinning at 1859 Hz. [b] T_1(C) relaxation for 65 ms. [c] Magic-angle spinning at 930 Hz. [d] T_1(C) relaxation for 25 ms. [e] T_1(C) relaxation for 250 ms.

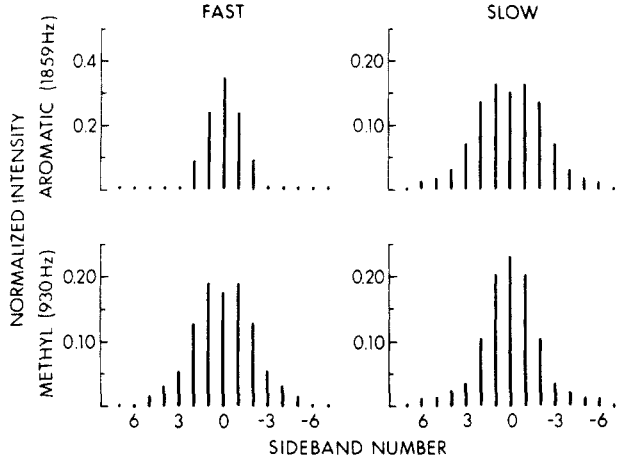

Figure 8. Dipolar ^1H–^{13}C Pake patterns for the protonated aromatic carbons (top) and methyl carbons (bottom) of the phenoxy resin, PK. The paterns on the left arise from the 50% of carbons with faster T_1(C) relaxation rates and those on the right from the 50% with slower relaxation rates. The faster relaxing methyl carbons have the broader dipolar patterns, opposite to the situation for the aromatic carbons.

This is not the situation for PK, however. The population in PK with shorter aromatic carbon T_1's has a narrower dipolar line shape, while that with longer aromatic carbon T_1's has a broader dipolar line shape (Figure 8, top). Furthermore, the chemical-shift tensors of the nonprotonated aromatic carbons, which are on the C_2 axes of the rings, are not averaged by the motion reducing dipolar coupling and producing the short ring T_1(C) in PK (Table IV). This result is only consistent with the presence of ring 180° flips as the dominant large-amplitude motion[6] for the 50% of the PK ring population with a short aromatic carbon T_1. The methyl carbon dipolar line shape is also sensitive to selection by T_1(C), except that for the methyl carbons, the broader dipolar pattern goes with the population with the shorter T_1(C) (Figure 8, bottom), opposite to the pairing observed for the aromatic carbons (Table III).

Discussion

Nature of the Motion. Several motions in PC and in PK can result in line narrowing of the proton resonance. Deuterium NMR[2] and ^{13}C–^1H dipolar spectra taken at room temperature[6] both indicate that essentially all of the phenylene groups are executing 180° rotations (flips) in PC. While it is reasonable to suppose that the narrowing in the PC resonance in the temperature region from −120 °C to just below room temperature is due partly to phenylene 180° flips, it has been pointed out before[30,31] that such flips modulate neither the interaction of the H2–H3 proton pair on the phenylene ring nor the interaction of the H3–H5 pair. However, the 180° phenylene flips will average inter-ring and inter-repeat-unit dipolar couplings. Since, the H3–H5′ distance across the carbonate linkage is only 40% greater than the H3–H5 intra-ring distance,[32] ring flips can have a significant effect on the proton line shape. Motions other than 180° phenylene flips will also narrow the PC proton line shape. As demonstrated both by ^2D NMR and ^{13}C–^1H dipolar spectra, these motions include phenylene torsional oscillations about the C1–C4 axis. Main-chain wiggles about other axes have been suggested by the ^{13}C–^1H dipolar spectra of the methyl carbons[6] but have not been reported in ^2D NMR studies. In short, we attribute the proton narrowing about equally to all three motions: large-amplitude phenylene 180° flips that significantly reduce inter-ring ^1H–^1H dipolar couplings and small-amplitude torsional oscillations and main-chain reorientations that partially reduce both inter- and intra-ring ^1H–^1H couplings.

Table IV
Intensities of Sidebands from Chemical Shift Anisotropies at 50.3 MHz for Nonprotonated Aromatic Carbons of PK Adjacent to the Isopropylidene Moiety, with Magic-Angle Spinning at 650 Hz

system	sideband number 2	1	0	−1	−2	−3
total sample	0.14	0.83	1.00	0.54	0.40	0.09
slowest 50%, T_1(C) selection	0.15	0.88	1.00	0.52	0.36	0.09

Pressure Dependence. The effect of pressure on the motions responsible for narrowing the proton resonance demonstrates the important role played by chain packing.

The activation volumes in Table I (20 and 25 cm^3/mol) are about 10% of the repeat-unit volumes. This means that large-volume fluctuations are not responsible for motions in PC and PK such as phenylene ring

flips but rather volume fluctuations which are, on average, only one-fourth to one-third of that of a single phenylene ring of the repeat unit. Of course, in such a heterogeneous system as a glassy polymer, distributions of activation and fluctuation volumes are present.

Boyer[33] has estimated the activation volume of the γ relaxation process from the mechanical data of Christiansen et al.[34] In essence, PC was found to become brittle at room temperature under a pressure 10 000 bars. This result was interpreted as due to the γ mechanical loss peak at 1 Hz moving from −100 °C at ambient pressure to near room temperature under 10 000 bars. Using the analysis leading to eq 6 and the data of Christiansen et al., we estimate an activation volume of 35 cm^3/mol, in reasonable agreement with the Table I value. We take the agreement as evidence that the γ mechanical loss peak and the proton line narrowing are both controlled by the same physical process. We also note that the activation energies deduced from proton NMR in PC and PK are in the same ratio (1.1) as the temperatures of maximum mechanical loss (1.2), to within experimental uncertainties. This similarity also supports the argument that the proton narrowing and the mechanical loss reflect the same motions. A lattice bundle-model description of these motions and their pressure dependence is presented in the last two sections of this Discussion.

Excess Volume in PC and PK. The density of quenched PC is between 1.16 and 1.20[35] while the density of a reasonable crystalline analogue, 4,4′-isopropylidenediphenylbis(phenyl carbonate), is 1.31.[32] Thus, the glassy polymer has about a 13% excess volume. The ^{13}C–^{1}H dipolar spectra demonstrate that nearly all of the phenylene units in PC execute 180° flips at a rate greater than 10^4 s^{-1} at room temperature,[6] while ^{2}D NMR experiments by Henrichs and Luss[36] have shown that none of the rings flip in this crystalline analogue. Evidently, the excess volume is important in allowing the phenylene groups to reorient. We have measured the density of PK as 1.24, which is 7% greater than that of polycarbonate. With the assumption that crystalline PK would also have a density of 1.31, PK has an excess volume of 6%. On this basis, one expects the phenylene flips to be less frequent in PK than in PC. Indeed, analysis of the results of Figure 8 indicates that only half of the phenylene groups in PK at room temperature are flipping faster than 10^4 s^{-1}. This conclusion also correlates with the higher temperature of the mechanical loss peak and the higher activation energy for PK observed by proton line narrowing in Table I, the latter reflecting the shift of the narrowing region to higher temperature in PK. Hence the relative excess volumes of PC and PK are in qualitative accord with the observations of motion in the two polymers. Finally, Henrichs and Luss have observed ring flips by ^{2}D NMR in a second crystal form of 4,4′-isopropylidenediphenylbis(phenyl carbonate).[36] The mobile form has a density of 1.240 compared to 1.308 for the immobile form.[37]

PC and PK Relaxation. The tighter packing in PK relative to that in PC increases the energy (or, equivalently, slows down the rate) of the main-chain wiggling and lattice distortions necessary for ring flips. Slowing down the rate of main-chain wiggling, which in PC is near 10^6 Hz at 25 °C,[6] increases the $T_{1\rho}(C)$ relaxation rate in PK, shortening the $T_{1\rho}(C)$'s relative to those in PC. The diversity of lattice sites in PK (some with and some without enough room to permit ring flips) is reflected in the greater width of the pressure-dependent T_2 process relative to that in PC (see Figures 1 and 3) as well as in the increased nonlinearity of methyl carbon $T_{1\rho}$ relaxation (Figure 7).

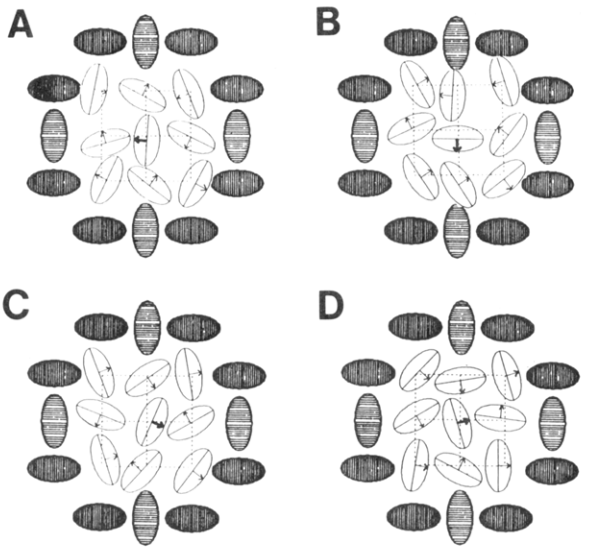

Figure 9. Schematic drawing of the packing of a few polycarbonate chains in a bundle. The two-dimensional matrix of ellipsoids represents rings that are lying in a plane perpendicular to the long axis of the bundle. The dark ellipsoids form a dynamic boundary whose motions are on a longer time scale. The time evolution of a 180° flip of the central ring proceeds from (A) to (D) and involves cooperative translations and rotations of the other rings of the bundle (adapted from Perchak, Skolnick, and Yaris, ref 38).

The packing is sufficiently tight in PK that interchain steric interactions are responsible for slowing down subnanosecond methyl-group C_3 rotation. This means that the most efficient methyl-group T_1 relaxation occurs for chains that are the most tightly packed. The most tightly packed chains have the least wiggling, the least motionally averaged ^{1}H–^{13}C dipolar coupling, and hence the broadest dipolar pattern (Figure 8, bottom). On the other hand, since the ring-flip process is itself an important contributor to the aromatic carbon T_1 in PK and since ring flips do not occur for that part of the population that is tightly packed, the most efficient T_1 aromatic carbon relaxation occurs for more loosely packed chains that are associated with a narrow ^{1}H–^{13}C dipolar pattern (Figure 8, top), opposite to the situation for the methyl carbons.

Bundle Model for Ring Flips. The notion that interchain packing is responsible for the steric constraints leading to 180° flips for the rings in polymers like PC and PK has been tested by computer simulations of chain dynamics.[38] In these simulations, chains were assumed to form bundles or regions over which main chains were locally parallel. No long-range periodicity was assumed. The important interchain correlation was considered to be transverse to the main-chain axis. This interaction was modeled by a two-dimensional matrix of ellipsoids representing rings from different chains lying in a plane perpendicular to the long axis of the bundle (Figure 9). Making reasonable assumptions about the nature of the inter-ring steric potential,[38] two necessary conditions for the existence of thermally activated 180° flips were established by the computer simulation. First, the centers of gravity of the ellipsoids representing the aromatic rings had to be allowed to move. If they were fixed, the rings could oscillate but not flip. Since we are considering motions below T_g, motion of the centers of gravity of the ellipsoids is equivalent to main-chain reorientation. Second, the bundle had to be surrounded by a boundary.

This boundary could be produced by steric interactions with rings in adjacent bundles (the dark ellipsoids in Figure 8) that may be moving but at substantially slower rates. If the boundary were removed (which might describe the situation in the melt or in solution), the rings in the central 3 × 3 bundle became free rotors. In times of the order of the time between flips (10 μs), the identification of a particular ring as part of a central bundle, or part of a boundary, would change. Chains in bundles are dynamically correlated and not permanently aligned.

Dynamic Correlations within PC and PK Bundles. We can interpret the pressure-induced clamping of motion in PC and PK in terms of removal of excess volume within the polymer bundles pictured in Figure 9. The increase in pressure squeezes the dark rings in the 3 × 3 matrix, and this densification inhibits the translations of the centers of gravity of the rings and so blocks the ring-flip process and inhibits ring oscillation and chain wiggling. The energy of activation of the ring-flip process is therefore that of the lattice reorganization. Thus, approximately 40 kJ/mol activation energies are measured both in mechanical-loss experiments[39] and in the experiments reported here and other solids NMR experiments.[5] The fact that the activation volumes are nearly the same for both PC and PK (Table I) fits within this description: The rings are the same size and so require the same molecular volume for clearance. This volume can be generated either by small translations and rotations of a large number of cooperating chains in a big bundle or by larger translations and rotations of a fewer number of chains in a small bundle. Since the activation volumes in PC and PK are nearly the same, even though the mobilities of the rings and chains are different, the volume required for ring flips is more likely generated by cooperative main-chain reorientations of only a few chains in a small bundle. The dynamic cooperativity of a large number of PK rings and chains is improbable because so many of them are immobile. The reversiblity of the pressure-induced line broadening is consistent with a minor reorganization of just a few nearest-neighbor chains in a confined volume.

We believe the 3 × 3 matrix pictured in Figure 9 is reasonable for the description of the dynamics of chain packing in both PC and PK. Motion of about half of the nine rings in such a matrix is probably critical for generation of the dilation preceding the flip. Computer simulations of chain motions in the melt have also suggested that transverse dynamic correlations are short range involving only a few chains,[40] a conclusion we believe to be true for the glass as well. Interchain steric interactions in PC may involve the isopropylidene and carbonate groups as well as the rings.

Acknowledgment. This work was supported by NSF Grants DMR 85-20789 and DMR 87-02847 and the generosity of the donors to the Petroleum Research Fund, administered by the American Chemical Society. We thank Joel Garbow (Monsanto Co., St. Louis, MO) for performing the slow-speed magic-angle spinning experiments, the results of which are reported in Table IV.

References and Notes

(1) Nielsen, L. E. *Mechanical Properties of Polymers*; Reinhold: New York, 1962; p 125.
(2) Spiess, H. W. *Colloid Polym. Sci.* **1983**, *261*, 193.
(3) Inglefield, P. T.; Amici, R. M.; Hung, C.-C.; O'Gara, J. F.; Jones, A. A. *Macromolecules* **1983**, *16*, 1552.
(4) Schaefer, J.; McKay, R. A.; Stejskal, E. O.; Dixon, W. T. *J. Magn. Reson.* **1983**, *52*, 123.
(5) Roy, A. K.; Jones, A. A.; Inglefield, P. T. *Macromolecules* **1986**, *19*, 1356.
(6) Schaefer, J.; Stejskal, E. O.; McKay, R. A.; Dixon, W. T. *Macromolecules* **1984**, *17*, 1479.
(7) Schaefer, J.; Stejskal, E. O.; Perchak, D.; Skolnick, J.; Yaris, R. *Macromolecules* **1985**, *18*, 368.
(8) Liu, N.-I.; Jonas, J. *J. Magn. Reson.* **1975**, *18*, 444.
(9) Assink, R. *J. Polym. Sci., Polym. Phys. Ed.* **1974**, *12*, 2281.
(10) Van Krevelen, D. W. *Properties of Polymers*; Elsevier: New York, 1976; pp 405–406.
(11) Schaefer, J.; Stejskal, E. O. *Top. Carbon-13 NMR Spectrosc.* **1979**, *3*, 284.
(12) Stejskal, E. O. U.S. Patent 4 446 430, May 1984.
(13) Torchia, D. A. *J. Magn. Reson.* **1978**, *30*, 613.
(14) Schaefer, J.; Sefcik, M. D.; Stejskal, E. O.; McKay, R. A. *Macromolecules* **1984**, *17*, 1118.
(15) Munowitz, M. G.; Griffin, R. G. *J. Chem. Phys.* **1982**, *76*, 2848.
(16) Burum, D. P.; Linder, M.; Ernst, R. R. *J. Magn. Reson.* **1981**, *44*, 173.
(17) Droste, D. H.; DiBenedetto, A. T. *J. Appl. Poly. Sci.* **1969**, *13*, 2149.
(18) Bracewell, R. N. *The Fourier Transform and Its Applications*, McGray-Hill: New York, 1986; p 41.
(19) McCall, D. W.; Falcone, D. R. *Trans. Faraday Soc.* **1970**, *66*, 262.
(20) Davenport, R. A.; Manuel, A. J. *Polymer* **1977**, *18*, 577.
(21) Zoller, P. *J. Poly. Sci., Polym. Phys. Ed.* **1982**, *20*, 1453.
(22) Kittel, C. *Introduction to Solid State Physics*, 4th Ed.; Wiley: New York, 1971; p 647.
(23) Bloembergen, N.; Purcell, E. M.; Pound, R. V. *Phys. Rev.* **1948**, *73*, 679.
(24) Flynn, C. P. *Point Defects and Diffusion*; Clarendon: Oxford, 1972; pp 319–325, 414–418.
(25) Schaefer, J.; Stejskal, E. O.; Buchdahl, R. *Macromolecules* **1977**, *10*, 384.
(26) Schaefer, J.; Stejskal, E. O.; Steger, T. R.; Sefcik, M. D.; McKay, R. A. *Macromolecules* **1980**, *13*, 1121.
(27) Gullion, T.; Schaefer, J. *J. Chem. Phys.*, in press.
(28) Cheung, T. T. P.; Yaris, R. *J. Chem. Phys.* **1980**, *72*, 3604.
(29) Schaefer, J.; Sefcik, M. D.; Stejskal, E. O.; McKay, R. A. *Macromolecules* **1981**, *14*, 280.
(30) Inglefield, P. T.; Jones, A. A.; Lubianez, R. P.; O'Gara, J. F. *Macromolecules* **1981**, *14*, 288.
(31) O'Gara, J. F.; Jones, A. A.; Hung, C.-C.; Inglefield, P. T. *Macromolecules* **1985**, *18*, 1117.
(32) Perez, S.; Scaringe, R. P. *Macromolecules* **1987**, *20*, 68.
(33) Boyer, R. F. In *Polymeric Materials. Relationships Between Structure and Mechanical Behavior*; American Society for Metals: Metals Park, 1975; p 308.
(34) Christiansen, A. W.; Baer, E.; Radcliffe, S. E. *Phil. Mag.* **1971**, *24*, 451.
(35) Chan, A. H.; Paul, D. R. *Poly. Eng. Sci.* **1980**, *20*, 87.
(36) Henrichs, P. M.; Luss, H. R. *Macromolecules* **1988**, *21*, 860.
(37) Henrichs, P. M.; Luss, H. R.; Scaringe, R. P. *Macromolecules* **1989**, *22*, 2731.
(38) Perchak, D.; Skolnick, J.; Yaris, R. *Macromolecules* **1987**, *20*, 121.
(39) Yee, A. F.; Smith, S. A. *Macromolecules* **1981**, *14*, 54.
(40) Kolinski, A.; Skolnick, J.; Yaris, R. *Macromolecules* **1986**, *19*, 2550.